J. Fluid Mech. (2012), *vol.* 702, *pp.* 5–25. © Cambridge University Press 2012
doi:10.1017/jfm.2012.94

The onset of fragmentation in binary liquid drop collisions

C. Planchette[1]†, E. Lorenceau[1]‡ and G. Brenn[2]

[1] Laboratoire de Physique des Matériaux Divisés et des Interfaces (LPMDI), Université Paris - Est, 5 boulevard Descartes, 77454 Marne-la-Vallée CEDEX 2, France

[2] Institute of Fluid Mechanics and Heat Transfer, Graz University of Technology, Inffeldgasse 25/F, 8010 Graz, Austria

(Received 7 July 2011; revised 23 December 2011; accepted 13 February 2012; first published online 1 May 2012)

Binary collisions of drops of immiscible liquids are investigated experimentally at well-defined conditions of impact. In the experiments we vary all relevant properties of an aqueous and an oil phase, the impact parameter, the drop size and the relative velocity. The drops observed after the collisions exhibit three main phenomena: full encapsulation, head-on fragmentation, and off-centre fragmentation. The regimes characterized by these phenomena replace the ones observed in binary collisions of drops of the same liquid: coalescence, reflexive separation, and stretching separation. Our aim is a universal description of the two fragmentation thresholds of such collisions. Based on the capillary instability and an energy balance, we establish for head-on collisions a scaling law for the evolution of the threshold impact velocity with the properties of the liquids and the droplet size. The fragmentation threshold for off-centre collisions is compared to established models from the literature, which appear unsatisfactory. Introducing an effective impact parameter, which accounts empirically for the deformation and rotation of the drops upon impact, we describe this fragmentation threshold in a universal way. For both fragmentation thresholds, the agreement between experimental data and their theoretical representation is very good. Our work yields new insight into binary collisions of drops and proposes a perspective to develop a more general description with implications for binary collisions of drops of a single liquid as well.

Key words: breakup/coalescence, drops, multiphase flow

1. Introduction

The first investigations of binary water drop collisions were triggered by meteorological interest for their importance in rainfall (Brazier-Smith, Jennings & Latham 1972). Technical interest in spray combustion and spray drying motivated investigations on the stability behaviour of colliding drops and the outcome from

† Present address: Research Center for Pharmaceutical Engineering, Inffeldgasse 21a/II, 8010 Graz, Austria. Email address for correspondence: carole.planchette@gmail.com

‡ Present address: Laboratoire Navier, UMR 8205, CNRS, Université Paris - Est, 2 allée Képler, 77420 Champs-sur-Marne, France.

https://doi.org/10.1017/jfm.2012.94 Published online by Cambridge University Press

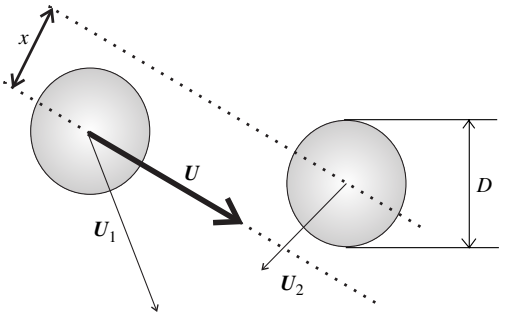


FIGURE 1. Geometric and kinetic parameters of binary drop collisions.

the drop collisions for liquids other than water also (Ashgriz & Poo 1990; Jiang, Umemura & Law 1992; Qian & Law 1997; Willis & Orme 2000; Brenn, Valkovska & Danov 2001; Gotaas *et al.* 2007). In all these studies, the colliding drops consisted of the same liquid. More recently, investigations on collisions of drops consisting of different, in part immiscible, liquids have begun (Gao, Chen & Lin 2005; Chen & Chen 2006; Chen 2007; Planchette, Lorenceau & Brenn 2010). The fields of technical applications of this kind of drop collision may range from combustion in engines to production processes in some life sciences, such as the coating of a liquid core by another, immiscible liquid. In the latter field, encapsulating one liquid within another one can be useful, for example, for the production of double emulsions. These allow the packaging and stabilizing fluids or their active ingredients within a protective shell. Double emulsions, which are typically made via two-step emulsifying processes or with microfluidic techniques (Goubault *et al.* 2001; Okushima *et al.* 2004; Utada *et al.* 2005; Chu *et al.* 2007), are usually obtained in a liquid phase. The collisions of immiscible liquid drops, as described in this article, can circumvent this limitation, since the emulsions can then be obtained in air.

For colliding drops of the same liquid in the special case of equal-sized drops, the collision outcome is determined by the diameter D and the relative velocity U of the two colliding drops, the impact parameter x of the collision (illustrated in figure 1), and by the density ρ, dynamic viscosity μ, and surface tension σ of the droplet liquid with respect to the ambient air. The outcome of the collision may therefore be represented in a non-dimensional form as depending on the non-dimensional impact parameter $X = x/D$, and, classically, on the Weber We and Ohnesorge Oh numbers, $\rho U^2 D/\sigma$ and $\mu/\sqrt{\sigma D \rho}$, respectively. It is important to note that this set of numbers, preferred in the state-of-art literature, is not the only possible one. An alternative is to represent the evolution of the Reynolds number $\rho UD/\mu$ with the Ohnesorge number.

Following the classical approach, the outcome of a collision with a given Ohnesorge number may be represented in the form of a nomogram (X, We). Four possible regimes (coalescence, bouncing, stretching separation, and reflexive separation) may be identified in the (X, We) nomogram for the head-on ($X \approx 0$) and the off-centre ($X \neq 0$) cases, as shown in figure 2 (Qian & Law 1997). In their study of collisions of equal-sized drops of the immiscible liquids diesel oil and water, Chen & Chen (2006) found the same regimes of outcomes of the collisions, characterized by the non-dimensional impact parameter X and the Weber number We based on the properties of the diesel oil. The shapes of the regimes in the (X, We) nomogram are very similar to the ones found, e.g. by Qian & Law (1997) in single-fluid drop collisions. As a difference,

https://doi.org/10.1017/jfm.2012.94 Published online by Cambridge University Press

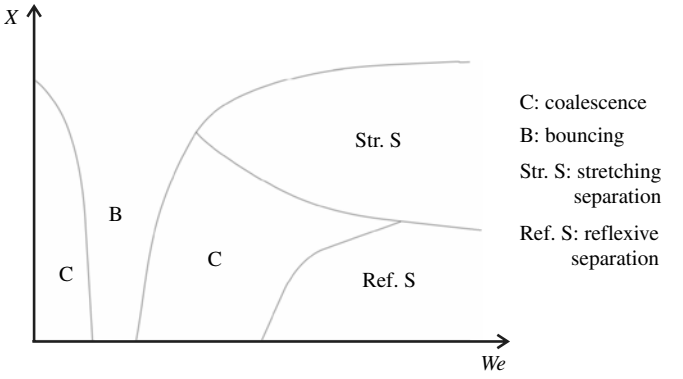


FIGURE 2. Sketch of the stability nomogram for binary drop collisions, where $We = \rho U^2 D/\sigma$ (adapted from Qian & Law 1997).

however, Chen & Chen (2006) found a mechanism which they termed 'single-reflex' separation. By this term they indicated that only the water drop is reflected from the plane of impact, while the diesel oil drop flows around the surface of the water drop and is, therefore, not reflected. In their work, Chen & Chen (2006) did not attempt to propose any model for the collision outcomes. In our work Planchette *et al.* (2010) we found an additional mechanism of immiscible liquid drop collisions which we termed 'crossing separation'. This mechanism consists of a motion of the oil phase on top of the aqueous drop, to the side opposite from the impact side, from where a drop of pure oil may pinch off. We will discuss these mechanisms in more detail in § 3 below.

In the studies of binary drop collisions known from the literature, a universal model allowing one to predict the collision outcome from the parameters of the problem (liquid properties, size and relative velocity of the drops, impact parameter) has not yet been developed. The introduction of two different immiscible liquids, which appears to be a problem of higher degree of complexity at first glance, has been found to be a powerful way to analyse the different phenomena taking place during the entire process. In this paper we propose to use this configuration to experimentally test the influence of the relevant parameters and develop satisfactory physical interpretations of the fragmentation thresholds. The potential to apply these findings to collisions of drops of a single liquid is one perspective of this work.

Our paper is organized as follows: we first present the set-up and materials used for the experimental part of the study. We continue by describing the main regimes of phenomena observed, comparing them to the ones for binary collisions of drops consisting of the same liquid. The two fragmentation thresholds for the head-on and the off-centre cases are then discussed. In § 4, we present a quantitative analysis for the threshold velocity of head-on collisions. The onset of fragmentation for off-centre collisions is discussed in § 5, where we introduce an effective impact parameter. In both cases, the experimental results and their theoretical interpretation are validated for a large range of parameters. The paper ends with the conclusions and a perspective of this study.

2. Experimental set-up and materials

2.1. *Experimental set-up and measuring techniques*

In order to produce well-defined collisions of two drops of immiscible liquids we use two droplet generators connected to two pressurized tanks, each containing one of the

https://doi.org/10.1017/jfm.2012.94 Published online by Cambridge University Press

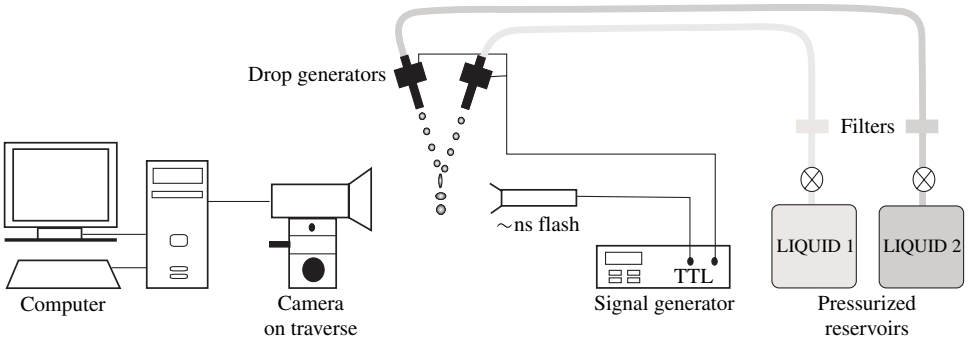


FIGURE 3. Experimental set-up with two droplet generators connected to two immiscible-liquid reservoirs. The generator positions can be adjusted with micro-control traverses. The ultrafast flash illuminates the colliding drops. Images are recorded by the camera.

two immiscible liquids, as represented in figure 3. Based on the controlled break-up of a laminar jet by the Rayleigh–Plateau instability, the droplet generators provide stable and monodisperse drop streams (Brenn, Durst & Tropea 1996). The nozzles can be changed for producing droplets of diameters ranging from 150 to 350 μm with a typical frequency of 10 kHz. For accurately adjusting the trajectories of the drops, the generators are fixed on translation and rotation stages. The accuracy of their displacements is estimated to be of the order of ± 2 μm and $\pm 2°$, respectively. The colliding droplets are illuminated by flashes of some nanoseconds duration. Images are recorded by a high-resolution PCO video camera Sensicam.

With the frequency of drop formation known, we deduce from these pictures all parameters needed for the description of the collisions: size and relative velocity of the drops, as well as the impact parameter. Indeed, since the formation of the drop streams is highly reproducible, pictures of several drop pairs generated at successive instants represent the time evolution of a given single pair of drops. The drop size D is obtained from the area A of the projection of the drop on the CCD array of the camera, using the equation $D = 2\sqrt{A/\pi}$. The resolution of our imaging system is 5 μm pixel^{-1}, which leads to an accuracy of the drop diameter measurement of ± 2 μm. The relative velocity and impact parameter are deduced from the relative positions of the drop centres of mass by vector calculation. Following this procedure, the accuracy is estimated to be of 1 %. In all of the pictures presented later in this paper, the elapsed time between two successive pairs of drops is 100 μs. The photographs always show droplets of 200 μm diameter. The dark liquid is a dyed aqueous solution of glycerol, while the transparent drops consist of oils. The relevant physical properties of the liquids are given in the next section.

2.2. *Immiscible liquids*

With the aim of achieving full encapsulation of one liquid by another one, we selected immiscible liquids showing total wetting properties.

The encapsulated phase is made of aqueous solutions of glycerol at various concentrations. As indicated in table 1, the viscosity of these solutions can be tuned from less than 2 mPa s to more than 10 mPa s without noticeable changes of the other parameters.

The encapsulating phase is an oil. We mainly use various silicon oils with viscosities ranging from 3 to 20 mPa s independently from the other properties.

https://doi.org/10.1017/jfm.2012.94 Published online by Cambridge University Press

Aqueous solutions % mass	Density kg m^{-3}	Dynamic viscosity mPa s	Surface tension mN m^{-1}	Interfacial tension mN m^{-1}
Glycerol 20 (G20)	1047.9	1.76	70.7	37.7[a]
Glycerol 30 (G30)	1072.9	2.50	70.3	36.7[a]
Glycerol 40 (G40)	1098.8	3.72	69.5	34.9[a]
Glycerol 50 (G50)	1126.0	6.00	68.6	34.8[a]
Glycerol 50 (G50)	1126.0	6.00	68.6	34.3[b]
Glycerol 55 (G55)	1139.0	7.90	68.1	33.8[a]
Glycerol 60 (G60)	1153.8	10.8	68	

TABLE 1. Properties of the aqueous glycerol solutions at 20 °C. Glycerol concentrations are given in mass per cent. Interfacial tensions correspond to oils [a] SO M3 and [b] SO M5.

Oils	Density kg m^{-3}	Dynamic viscosity mPa s	Surface tension mN m^{-1}	Interfacial tension mN m^{-1}	Spreading parameter mN m^{-1}
SO M3	892.2	2.79[a]	19.5[a]	34.9[b]	14.8
SO M5	913.4	4.57[a]	19.5	—	14.1
SO M5+10	925.3	6.6	19.8	—	13.8
SO M10	937.2	9.37[a]	20.1	—	13.5
SO M10+20	944.5	14.28	20.3	—	13.3
SO M20	951.8	19.0[a]	20.7	—	12.9
PERFLUO	1934.9	5.5[a]	17.8	36.5[b]	14.3

TABLE 2. Properties of the oils at 20 °C; + denotes mixtures of two oils. [a] Values given by the data sheet of our supplier Carl Roth. [b] Interfacial tensions are given for contact with a glycerol solution at 50 %.

A fluorinated oil (perfluorodecalin) is also used, which allows us to measure the effect of a density change. The properties of these oils are presented in table 2.

In this paper, the aqueous solutions are denoted by the subscript *water*, and the oils by the subscript *oil*. For all combinations we checked the total wettability of the aqueous solutions by the oils. Surface and interfacial tensions, measured with the pendant drop method (tensiometer LAUDA TVT-1) and listed in tables 1 and 2, show very little variation. The surface energy contribution is therefore always of the same order and is not addressed in detail in the theoretical part of our study.

3. Main regimes observed

As for the collisions of drops of the same liquid, nomograms can be constructed to qualitatively show regimes characterized by different phenomena after the collisions. In contrast to the classical collisions, we make the choice not to use the Weber number, but to replace it by the relative velocity U of the drops; the Weber number definition is no longer clear as two surface tensions and one interfacial tension coexist. Moreover, as we have mentioned already, the surface energy associated with the collisions of glycerol solution and silicon oil drops is always of the same order. This term is therefore not relevant for explaining the variations of fragmentation thresholds.

https://doi.org/10.1017/jfm.2012.94 Published online by Cambridge University Press

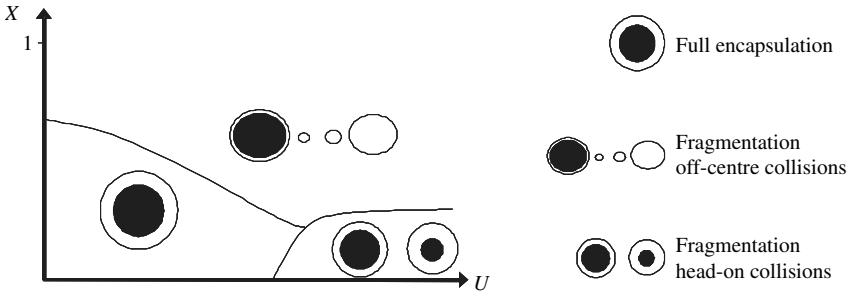


FIGURE 4. Typical (X, U) nomogram obtained for collisions of immiscible liquid drops. Three main regimes are observed: full encapsulation, fragmentation for off-centre collisions, and fragmentation for head-on collisions. For the fragmented drops, the oil/water distribution (in the sketches white/black, respectively) can vary and is therefore not representative of all cases. A typical value of U at the onset of fragmentation for $X \approx 0$ is 2.5 m s^{-1}.

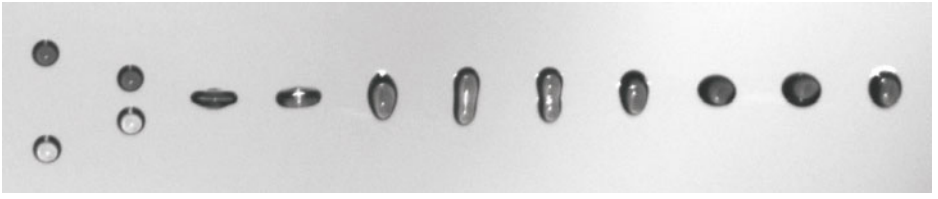


FIGURE 5. Full encapsulation of a 50 % glycerol solution drop by SO M20. The relative velocity of the drops at the impact is 3.88 m s^{-1}.

Such an (X, U) nomogram is presented in figure 4, where three main regimes are seen:

(i) *Full encapsulation* is seen for moderate impact parameters and moderate relative velocities. The oil droplet spreads on the aqueous one and fully remains around it, forming a liquid shell. Such an encapsulated drop is thus composed of an aqueous core coated by an oil film. The excess of energy resulting from the collision and leading to a strong distortion of the drops is dissipated, and the encapsulated drop finally assumes the expected spherical shape. Such an encapsulation is shown in figure 5. If the liquids were miscible, the regime of coalescence would replace the encapsulation.

(ii) For higher relative velocity and small impact parameter close to zero, *fragmentation for head-on collisions* is observed. The collision complex generated by the impact relaxes from a disk-like shape (actually we observe a thin lamella surrounded by a thicker rim) to a cylinder. Fragmentation is brought about by the break-up of the cylinder and generates two main drops. Depending on the combination of liquids, the distribution of the liquids in these two drops can vary. As we are not interested in this distribution in the present study, we limit our analysis to a description of the three typical cases. The so-called 'crossing separation' (Planchette *et al.* 2010) produces a single encapsulated drop plus a smaller pure oil drop ejected from the side opposite to the side of the original drop arrival. 'Single-reflex separation' (Chen & Chen 2006; Planchette *et al.* 2010) occurs when the aqueous drop is split, resulting in two encapsulated drops.

https://doi.org/10.1017/jfm.2012.94 Published online by Cambridge University Press

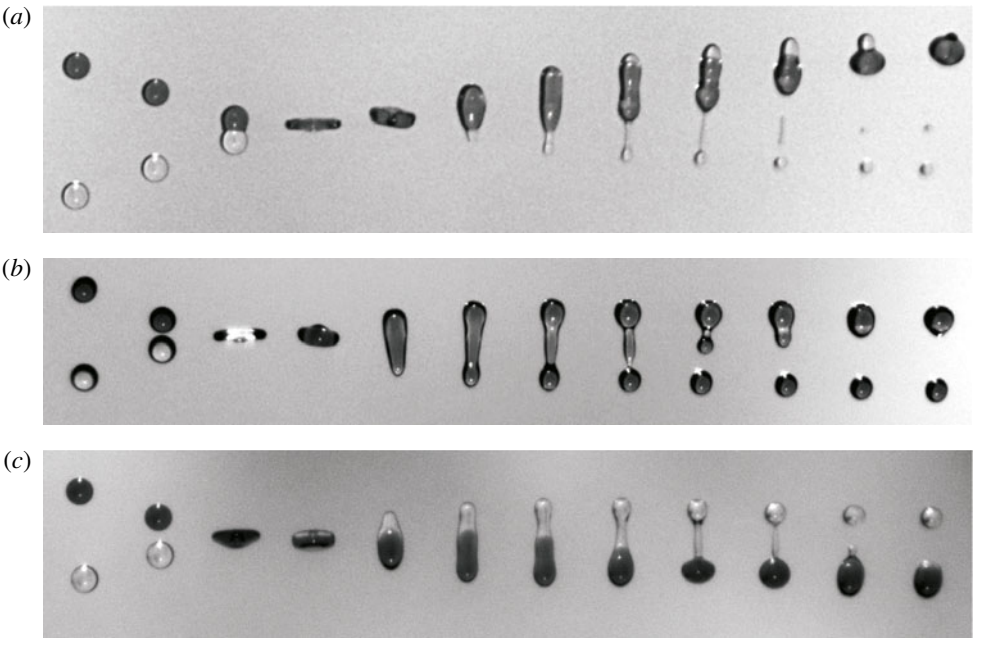


FIGURE 6. Examples of head-on fragmentation showing the three typical liquid distributions: (*a*) 'quasi-reflexive separation' (G50 and perfluorodecaline, $U = 3.95$ m s^{-1}), (*b*) 'single-reflex separation' (G20 and SO M10, $U = 4.32$ m s^{-1}), and (*c*) 'crossing separation' (G50 and SO M5, $U = 3.97$ m s^{-1}).

The relative distribution of the two liquids is unknown in this case. Finally, the 'quasi-reflexive separation' (Planchette *et al.* 2010) generates a single encapsulated drop plus a much smaller pure oil droplet located on the side of the original oil droplet approach. These three subclasses collected together under the term 'fragmentation for head-on collisions' are shown in the pictures of figure 6. Note that, when the liquids are miscible, we observe one single regime instead: reflexive separation. Owing to the symmetry of such a collision, the collision plane acts as a mirror, and the distribution of the liquids is almost unchanged by the temporary merging of the two drops.

(iii) The third and last regime, found for high impact parameter and any relative velocity, is *fragmentation for off-centre collisions*. Owing to the eccentricity of the collisions, the volume of interaction of the two drops is limited and quickly turned into a liquid bridge connecting the two spherical caps which do not strongly interact. These caps continue to move apart on their original trajectories, forcing the liquid ligament to be stretched until it breaks up into small satellite droplets. The typical result of this regime includes two main drops: an aqueous drop covered by a thin layer of oil and a pure oil drop of a comparable size (note that sometimes some additional satellite droplets, mainly consisting of oil, are formed by the break-up of the oil filament). Here, again, the distribution of the liquids can vary with the combination of liquids and the impact parameter. Some illustrations of this regime – similar to stretching separation for collisions of drops of the same liquid – can be seen in figure 7.

https://doi.org/10.1017/jfm.2012.94 Published online by Cambridge University Press

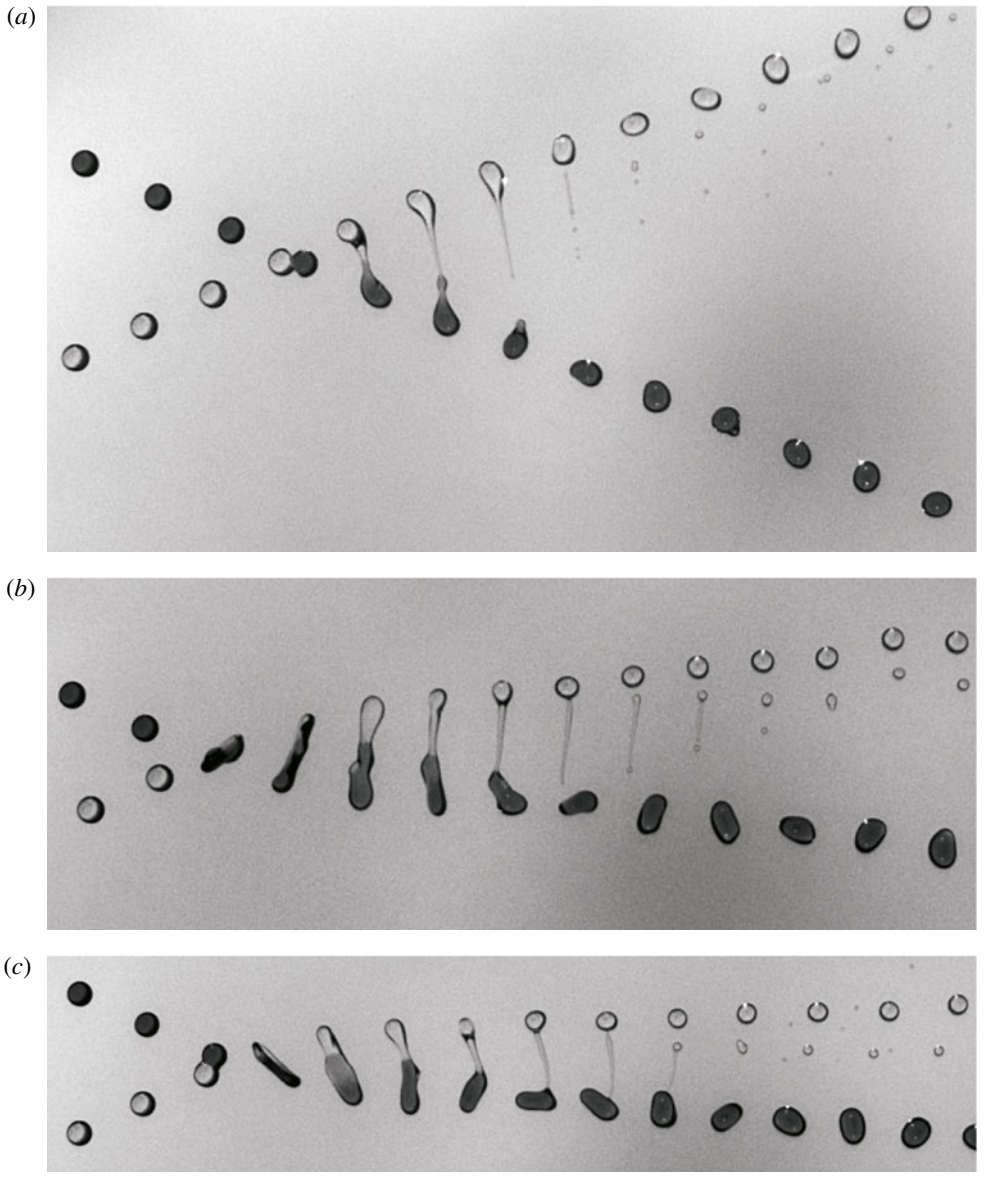


FIGURE 7. Examples of off-centre fragmentation for collisions of G50 and SO M5 drops. The impact velocity is 5.07 m s^{-1}, the impact parameter decreases from top to bottom: (*a*) 0.81, (*b*) 0.42, and (*c*) 0.33.

For head-on collisions, the full encapsulation and fragmentation regimes are defined by the threshold velocity U_c. This velocity is experimentally obtained as the mean of the highest and lowest velocities leading to full encapsulation and fragmentation, respectively. The typical uncertainty in U_c is less than ± 0.1 m s^{-1}.

In contrast to collisions of drops of miscible liquids, we do not observe a bouncing regime. This, however, has been observed for immiscible liquids under different experimental conditions elsewhere (Chen & Chen 2006). The colliding drops studied

https://doi.org/10.1017/jfm.2012.94 Published online by Cambridge University Press

by those authors consisted of water and diesel oil, they were equal-sized at diameters between 700 and 800 μm, and they collided at relative velocities between 0.6 and 2 m s^{-1}. Drop sizes and velocities were determined by image processing. The reason for our experimental finding may be, on the one hand, that our drops are much smaller than the ones realized by Chen & Chen (2006), and, on the other hand, their higher relative velocities. Actually, there is a factor of four in the typical diameters of the drops, and a factor of two in the minimum relative velocities of their study and ours. Bouncing being often attributed to the incomplete drainage of an air cushion between the two interfaces (Vincent *et al.* 2007), reaching the bouncing regime with our combination of liquids may require bigger drops and smaller relative velocities than investigated here. The focus of our present experiments, rather, lies on the fragmentation of drops after merging.

Looking at the nomogram of figure 4, the problem of understanding and describing the transitions between the regimes naturally arises. For head-on collisions, the question can be formulated as 'how large is the threshold velocity between full encapsulation and fragmentation?' A plausible answer is developed in the next section, where a scaling law representing the experimental data over wide ranges of the experimental parameters is established theoretically. The case of off-centre collisions is treated in § 5.

4. Head-on collisions: onset of fragmentation

In order to develop an analytical expression for the threshold velocity U_c between full encapsulation and fragmentation for head-on collisions, we first develop a fragmentation criterion. This criterion emerging from surface energy considerations and validated by experimental observation is presented in § 4.1. We then divide the collision into two main processes, allowing us to relate our fragmentation criterion to the initial state of the drops. The first phase corresponds to the deformation of the drops by the impact. It lasts until the collision complex has reached its maximum extension and the shape of a flat disk. Because of the analogy between a drop and a spring (Richard, Clanet & Quéré 2002; Okumura *et al.* 2003; Biance 2004), we will refer to this phase as the 'compression phase', noting nonetheless that the liquids do not undergo any compression themselves. A second phase follows, where this liquid 'disk' relaxes, forming a liquid cylinder. The associated energy losses are discussed in §§ 4.2 and 4.3. The theoretical expression for U_c is finally compared to the experimental results.

4.1. *Fragmentation criterion*

The fragmentation of the liquid cylinder formed after the collision, which produces two drops of almost equal size, suggests a mechanism similar to the one observed for a static cylinder and known as the Rayleigh instability. Once the length-to-diameter (aspect) ratio exceeds the critical value of π, a liquid cylinder breaks up into equal-sized drops, minimizing the total surface energy. This mechanism of fragmentation has already been considered in Ashgriz & Poo (1990) for binary collisions of water drops undergoing reflexive separation. Finite cylinders at much larger aspect ratios may be subject to a different instability mechanism, such as end-pinching.

To validate such a fragmentation criterion, we measure the aspect ratios $\zeta_p = b/a$ of the liquid cylinders on the recorded images. A schematic for the definition of ζ_p is shown in figure 8. The values are collected for several glycerol concentrations, and the relative velocity of the drops is varied including regimes of both encapsulation and fragmentation.

https://doi.org/10.1017/jfm.2012.94 Published online by Cambridge University Press

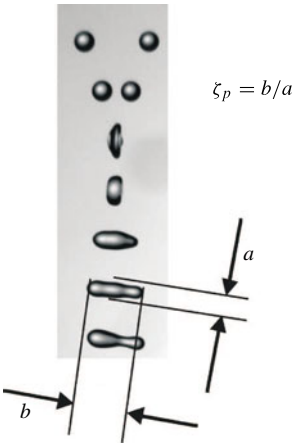


FIGURE 8. Definition of ζ_p, the aspect ratio of the liquid cylinder resulting from the collision.

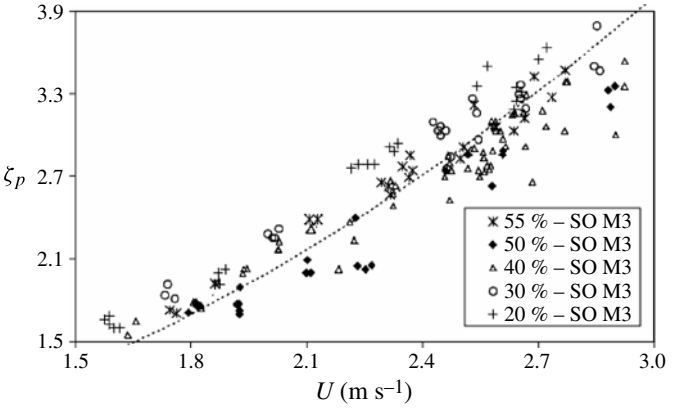


FIGURE 9. Evolution of ζ_p with the relative velocity of the drops at impact for different glycerol concentrations. The viscosity ranges from 1.8 to 7.9 mPa s. The oil was SO M3 in all cases. All data points are distributed along a single curve. The fit curve corresponds to $\zeta_p = 0.4 + 0.4U^2$.

All these data are shown in the diagram presented in figure 9. Even though the glycerol solution viscosity ranges from less than 2 mPa s to almost 8 mPa s, all data points are distributed along a single curve. We then determine the critical aspect ratio $\zeta_{p,crit}$ corresponding to the transition from full encapsulation to fragmentation. As we see in figure 10, the critical aspect ratio is independent of the aqueous-phase viscosity. Moreover, the value of the order of three is very close to the Rayleigh value of π. This result is surprising: it suggests that there is no influence of the finite size of the cylinder, nor of the internal flow of the two liquids on the fragmentation mechanism. Yet, it has been shown that the fragmentation of a stretched liquid cylinder is completely different from the classical Rayleigh–Plateau break-up problem (Rayleigh 1879; Marmottant & Villermaux 2004; Notz & Basaran 2004; Tong & Wang 2007). In our case the break-up always occurs slightly before the maximum extension state of the liquid cylinder. In fact, the images of figure 6 shows that the liquid

https://doi.org/10.1017/jfm.2012.94 Published online by Cambridge University Press

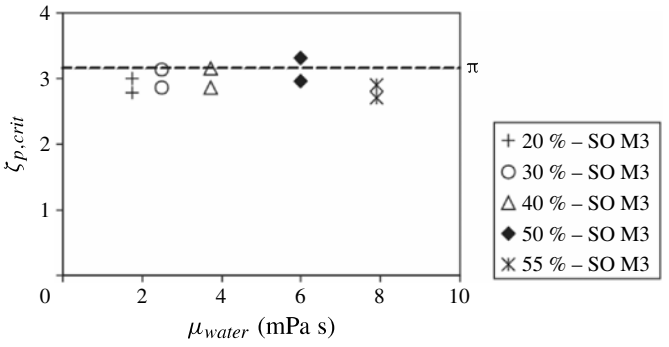


FIGURE 10. Evolution of $\zeta_{p,crit}$ with the viscosity of the glycerol solutions ranging from 1.8 to 7.9 mPa s. The oil was SO M3 in all cases. $\zeta_{p,crit}$ remains close to 3, in good agreement with the Rayleigh criterion, for which we expect the value of π.

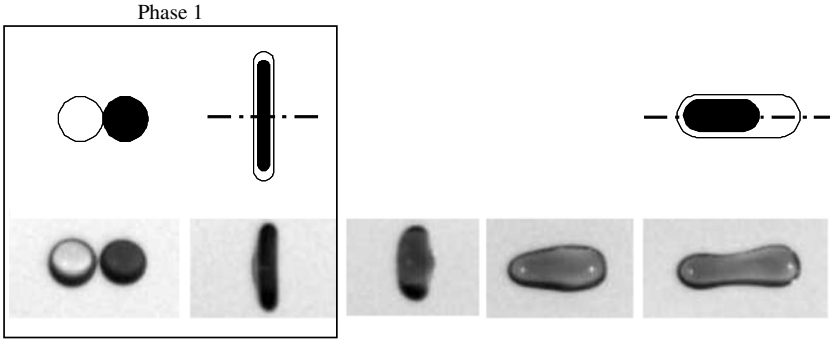


FIGURE 11. Structure of the collision process in two phases. Phase 1 (framed) lasts from the first contact until the complex reaches its maximum extension. The time between two successive pictures is 100 μs. The distribution of the two liquids in the case depicted here is not representative of all cases observed.

cylinder breaks up ~600–700 μs after the collision (6th or 7th position counted from the instant of first contact of the drops), which corresponds to the expected oscillation period for the base mode of the encapsulated drop with twice the volume of the colliding drops: $T = (\pi/4)\sqrt{(\rho_{oil} 2D^3/\sigma_{oil})} \approx 700$ μs. Thus, the internal flows within the liquid cylinder enhance the break-up, rather than preventing it.

These experimental results bring us to the following conclusions: the evolution of the liquid cylinder is independent of the viscosity of the encapsulated phase. For a given concentration of glycerol it can be described as a function of the relative velocity only. The fragmentation of the cylinder occurs when it reaches an aspect ratio of the order of three, which corresponds to the expected value of π given by the Rayleigh criterion. As a consequence, the velocity threshold between encapsulation and fragmentation is also found to be independent of the viscosity of the encapsulated phase.

In the next sections we focus on two successive phases of the collision with the aim of relating the fragmentation criterion established above to the initial kinetic energy using the intermediate state where the complex reaches its maximum extension.

https://doi.org/10.1017/jfm.2012.94 Published online by Cambridge University Press

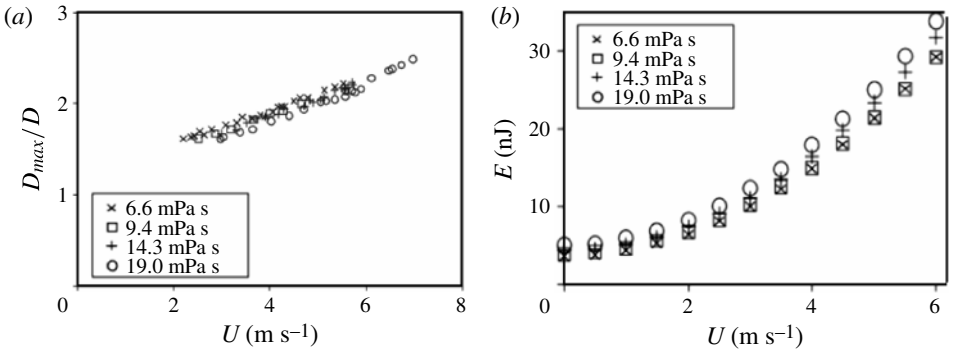


FIGURE 12. (*a*) Evolution of the maximum extension of the disk with the relative drop velocity U for different oils. The oil viscosity ranges from 6.6 to 19 mPa s, the glycerol concentration is constant (50 %). (*b*) Evolution of the energy loss E between the initial state and the disk at its maximum extension for the same combinations of liquids as in (*a*). E is found to be quasi-inertial, independent from the oil viscosity.

4.2. *Compression*

In this section we estimate the energy loss of the 'compression' phase, which turns the two drops into a thin lamella bounded by a rim as shown in figure 11. This structure looks like a disk in a side view (see e.g. figure 6). Knowing the initial kinetic and surface energies, we can also estimate the surface energy of the complex at its maximum extension to deduce the energy loss in this period. An accurate observation of the drops at the very early stage of the collision shows that the encapsulation of the aqueous core by the oil film is complete before the complex reaches its maximum extension. This suggests estimating the surface energy of the disk ($E_{\sigma\ disk}$) as

$$E_{\sigma\ disk} = \tfrac{1}{2}(\sigma_{oil} + \sigma_{water/oil})\pi D_{max}^2. \tag{4.1}$$

The temporal and spatial resolutions of our images allow us to measure the maximum diameter of the complex. This maximum diameter was estimated for several pairs of liquids and a wide range of velocities, independent from the regime observed (full encapsulation or fragmentation). Typical results are presented in figure 12(*a*).

We use these experimental results in combination with the following energy balance to deduce the energy loss E in this first period:

$$E = E_k + E_{\sigma\ ini} - E_{\sigma\ disk}. \tag{4.2}$$

In this balance, E_k and $E_{\sigma\ ini}$ are the initial kinetic and the initial surface energies, respectively. Obviously, $E_k = \pi\,(\rho_{water} + \rho_{oil})\,D^3U^2/48$ and $E_{\sigma\ ini} = \pi D^2\,(\sigma_{water} + \sigma_{oil})$.

As seen in figure 12(*b*), this loss is almost independent of the oil viscosity, since it rises only by a few per cent as the viscosity is increased by a factor of three. We also observe that the energetic loss increases as the velocity squared. This would suggest an inertial energetic loss, and normalizing this inertial part by the initial kinetic energy of the drops leads to the result that 94 % of the initial kinetic energy is lost. It is interesting to note that similar results have also been observed for binary collisions of drops of the same liquid by Jiang *et al.* (1992), and for the impact of drops on a solid surface by Eggers *et al.* (2010) and by Villermaux & Bossa (2011). In those symmetric impact situations at high Weber numbers, the flow is highly dissipative: while energy conservation would lead to $D_{max}/D \sim \sqrt{We/6}$, momentum conservation

https://doi.org/10.1017/jfm.2012.94 Published online by Cambridge University Press

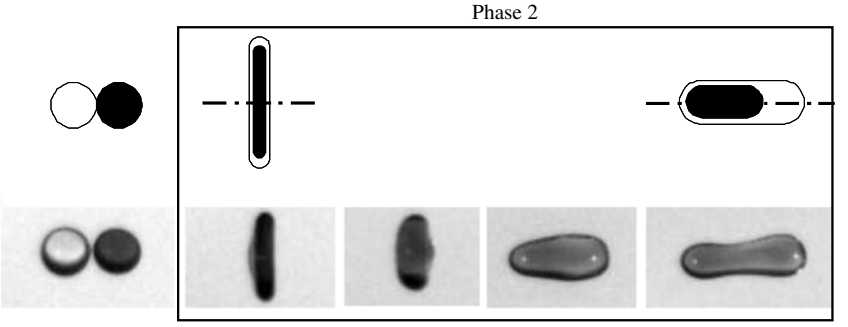


FIGURE 13. Structure of the collision process in two phases. In phase 2 (framed) the disk relaxes into a cylinder. The time between two successive pictures is 100 μs.

yields $D_{max}/D \sim 0.12\sqrt{We}$. Thus, the inertial loss measured when the drops reach the maximum extension can reach $1 - 6 \times 0.12^2 = 0.91$, which corresponds to 91 % of the initial kinetic energy, of the same order as observed for immiscible liquids. This inertial loss can be interpreted as a consequence of the formation of a rim where all the incoming kinetic energy of the drops absorbed in it is basically dissipated.

Thus, only 9 % of the initial kinetic energy is converted into surface energy when a single drop impacts a solid surface, while in the collision of two drops of immiscible liquids, our measurements show that only 6 % is available. These two values are very close despite the disparity in the geometry of the two experiments and reveal that the first phase of the collision is always highly dissipative. In the rest of this paper, we will therefore consider that only 6 % of the initial kinetic energy remains for the second phase of the collision. Moreover, as we already have a fragmentation criterion, the last step leading to an expression for the threshold velocity consists of describing this second phase.

4.3. *Relaxation of the disk*

The second phase of the collision corresponds to the relaxation of the disk into a cylinder, as illustrated in figure 13. As already mentioned, it is possible to make use of an analogy between a drop and a spring (Richard *et al.* 2002; Okumura *et al.* 2003; Biance 2004). More precisely, during its 'compression phase', the kinetic energy of the drop is partially transformed into surface energy. This excess of energy is then dissipated by the drop oscillation in the relaxation phase. This second phase can thus be treated as an analogue of the relaxation of a compressed spring, which will oscillate around its equilibrium position. For the drop collisions studied here, oscillations are strongly damped by the liquid viscosity, which leads to an aperiodic relaxation.

In this section, we aim to relate the complex at its maximum extension to the fragmentation criterion in order to finally establish a relation between the initial state of the drops and the threshold velocity U_c. As the encapsulation is complete when the disk reaches its maximum extension, we can consider that this relaxation phase corresponds to an aperiodic oscillation of an encapsulated drop. Indeed, excluding the contributions from surface energies, the energy balance of this second phase is reduced to

$$E_k - E = E_\mu \tag{4.3}$$

where E_μ is the viscous loss during the relaxation of the disk.

https://doi.org/10.1017/jfm.2012.94 Published online by Cambridge University Press

For estimating E_μ after the maximum extension phase we assume that the viscous loss is confined to the oil film, where the largest velocities are reached. This hypothesis is in good agreement with the experimental results presented in § 4.1, showing that the threshold velocity does not depend on the encapsulated-phase viscosity. In this oil film, the velocity gradients occur on a typical thickness $h \approx D$, thus yielding the expression

$$E_\mu \approx \mu_{oil} \left(\frac{V_{relax}}{h} \right)^2 \pi D^3 \frac{D}{V_{relax}} \approx \mu_{oil} \frac{V_{relax}}{D} \pi D^3 \tag{4.4}$$

for the viscous loss during the second phase of the impact, where V_{relax} is the relaxation velocity after the collision. It can be evaluated as proposed in Bartolo, Josserand & Bonn (2005) as $V_{relax} \approx L/\tau_i$, where $\tau_i \approx (D^3 \rho_{oil}/\sigma_{oil})^{1/2}$ corresponds to the capillary oscillation period of an inviscid droplet and L is the maximum extension of the drop. As a result, the energy dissipated by viscosity is

$$E_\mu = \mu_{oil} \sqrt{\frac{\sigma_{oil}}{\rho_{oil} D^3}} \pi D^3 \frac{L}{D}. \tag{4.5}$$

The viscous dissipation obtained is independent of the impact velocity U. This remarkable feature can be understood in the framework developed by Richard *et al.* (2002), Okumura *et al.* (2003), Clanet *et al.* (2004) and Biance *et al.* (2006) when considering the impact of a single drop on a solid surface: the rebound is globally considered as an oscillation. In this framework, the drop is a spring of stiffness σ and mass ρD^3, which oscillates with a period of the order of $(D^3 \rho/\sigma)^{1/2}$.

We then identify the ratio L/D as the aspect ratio of the cylinder ζ_p and balance the kinetic energy left after the expansion of the disk by this viscous loss. This yields

$$\mu_{oil} \sqrt{\frac{\sigma_{oil}}{\rho_{oil} D^3}} \pi D^3 \zeta_p = E_k - E = \frac{0.06\pi}{48} \left(\rho_{oil} + \rho_{water} \right) D^3 U^2. \tag{4.6}$$

We make use of the fragmentation criterion to finally obtain the threshold velocity U_c^{theo}. Indeed, we consider that the cylinder breaks up for $\zeta_p = \pi$. This leads to

$$U_c^{theo} = \sqrt{\frac{48\pi}{0.06} \frac{\mu_{oil}}{\rho_{oil} + \rho_{water}} \sqrt{\frac{\sigma_{oil}}{\rho_{oil} D^3}}}. \tag{4.7}$$

The scaling law thus established corresponds to a variation of the threshold velocity with μ_{water}^0, $\mu_{oil}^{1/2}$, and $D^{-3/4}$. These three powers obtained theoretically are very well confirmed by the experimental results shown in figure 14.

More generally, the whole of our data, plus the results by Chen & Chen (2006), are represented in figure 15 together with the theoretical evaluation of U_c^{theo}. This includes a wide range of combinations of liquids (glycerol solutions with viscosities ranging from 1.8 to 10.8 mPa s, silicon oils with viscosities varying from 2.8 to 19 mPa s, plus one fluorinated oil with double the density) and drop diameters from 150 to 350 μm. We emphasize that the agreement between these experimental results and the theoretical expression is very good: the slope between the experimental data and the theoretical prediction deduced from our analysis captures quantitatively the fragmentation mechanism since the straight line in figure 15, which corresponds to $U_c = U_c^{theo}$, is in perfect agreement with the data.

https://doi.org/10.1017/jfm.2012.94 Published online by Cambridge University Press

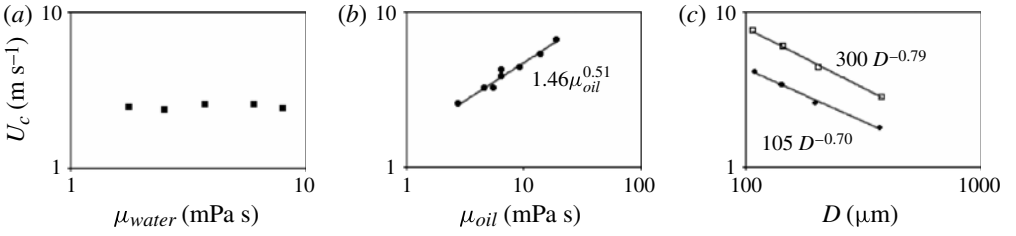


FIGURE 14. Evolution of the measured threshold velocity with (*a*) the aqueous solution viscosity ($\mu_{oil} = 2.79$ mPa s), (*b*) the oil viscosity ($\mu_{water} = 6$ mPa s), and (*c*) the drop diameter (aqueous phase G50, oil phase – upper line SO M10, lower line SO M3). The powers μ_{water}^{0}, $\mu_{oil}^{1/2}$, and $D^{-3/4}$ of the scaling law (4.7) are in very good agreement with the experimental data.

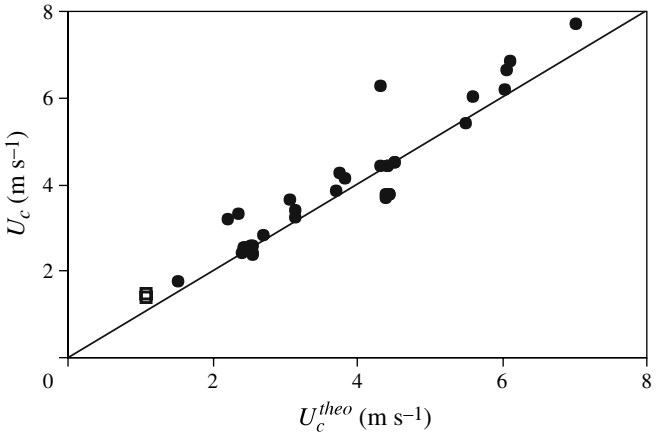


FIGURE 15. Comparison of the experimental threshold velocities with the theoretical values given by (4.7). All results are shown, including all liquids of tables 1 and 2 and the various drop diameters of figure 14 between 150 and 360 μm. The data corresponding to collisions of diesel oil and water drops of 750 μm diameter, extracted from Chen & Chen (2006), are also plotted (open squares). The straight line indicates $U_c = U_c^{theo}$.

4.4. *Conclusions on fragmentation after head-on collisions*

The above scaling law (4.7) can be reformulated using non-dimensional quantities such as the oil Ohnesorge and modified Reynolds numbers defined as $Oh_{oil} = \mu_{oil}/\sqrt{\sigma_{oil}\rho_{oil}D}$ and $Re = (\rho_{oil} + \rho_{water})\,DU_c/2\mu_{oil}$, respectively. We obtain

$$Re \approx \sqrt{\frac{\rho_{oil} + \rho_{water}}{\rho_{oil}}}\,Oh_{oil}. \tag{4.8}$$

This allows a direct comparison with results from the literature on binary collisions of drops consisting of the same liquid (Ashgriz & Poo 1990; Jiang *et al.* 1992; Qian & Law 1997; Estrade *et al.* 1998; Willis & Orme 2000; Brenn & Kolobaric 2006; Gotaas *et al.* 2007). The experimental results include various liquids, such as water, alkanes, propanol, octanol, glycol, and others, and different drop diameters. As we can see in figure 16, the scaling law established for immiscible liquids cannot be applied as such

https://doi.org/10.1017/jfm.2012.94 Published online by Cambridge University Press

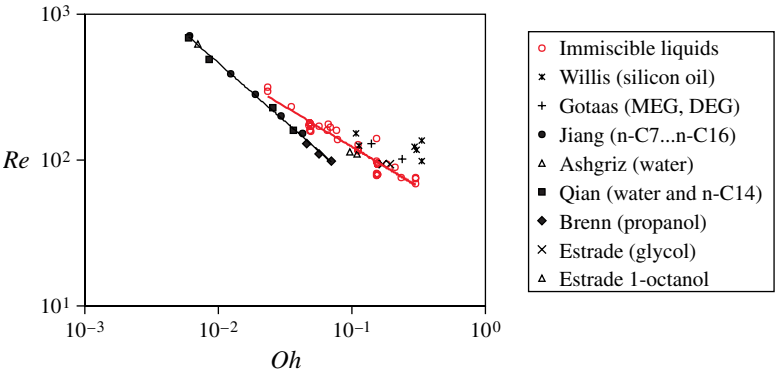


FIGURE 16. (Colour online available at journals.cambridge.org/flm) Representation of the scaling law (4.7) by *Re* and *Oh* (4.8). Literature data for collisions of drops of the same liquid are also shown (denoted by the first author only). Here 'Brenn' refers to Brenn & Kolobaric (2006). The behaviour is different and can be divided into two main regimes. A regime of strong dissipation, for high *Oh*, where the fragmentation occurs at constant *Re*. And a second regime at low *Oh*, where a power law between *Re* and *Oh* is obtained. The exponent is not the same as for the immiscible-liquid drop collisions, which can be explained by different flow fields in the drops.

to binary collisions of drops of the same liquid. Even though the data for immiscible and miscible collisions lie in the same ranges of *Re* and *Oh*, they do not collapse. We explain this difference by the fact that the viscous dissipation in the relaxation phase is not concentrated on an oil film any more. For collisions of miscible drops, two cases are observed instead. For high Ohnesorge number, when the relaxation time of the complex is small in comparison to the viscous dissipation time, we obtain a fragmentation limit corresponding to a constant Reynolds number. Indeed, in this case, the viscous dissipation can be written as $E_\mu \approx \mu(U/h)^2 D^2 h(D/U) \approx \mu U D^2$ which, balanced by the kinetic energy, yields the expected fragmentation limit. For low Ohnesorge number, a power law between *Oh* and *Re* appears. The exponent close to -0.8 is different from the one obtained for immiscible liquids. Here, again, the main flow field is not restricted to a coating any more, which can explain this difference.

Despite this aspect, we believe the approach presented in this paper for immiscible drop collisions, which structures the collisions into two successive periods and implements the Rayleigh-like criterion for fragmentation, can still be used for miscible drop collisions. As already mentioned, there is also an inertial energy loss in the first part of the collision. Moreover, the critical aspect ratio of the cylinder undergoing fragmentation is found to be of the order of π as used by Ashgriz & Poo (1990) for collisions of water drops also.

5. Off-centre collisions: onset of fragmentation

In this section we describe and interpret drop fragmentation for off-centre collisions. Two principal models of the literature (Brazier-Smith *et al.* 1972; Jiang *et al.* 1992), developed for binary collisions of drops of the same liquid and presenting the critical impact parameter X_{cr} as a function of the Weber number *We*, are tested with experimental results obtained for our immiscible liquid drops. We then propose an alternative to the classical interpretation, which fails to represent our data, taking into account the rotation and distortion of the drops through an effective impact parameter.

https://doi.org/10.1017/jfm.2012.94 Published online by Cambridge University Press

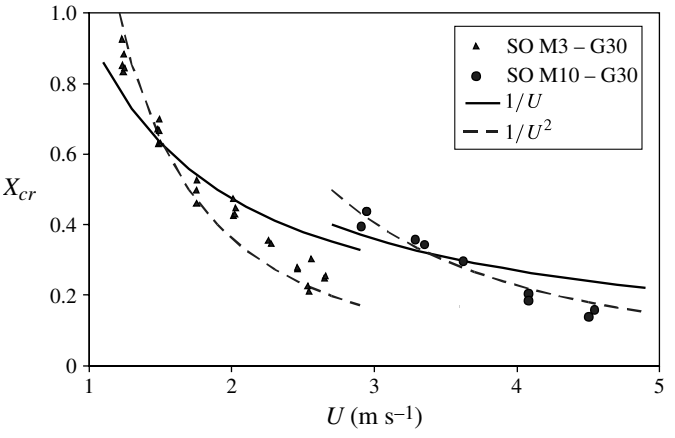


FIGURE 17. Evolution of the critical impact parameter X_{cr} with the velocity U for different liquid combinations. The corresponding representations based on (5.1) and (5.2) are also shown. Neither of the two scaling laws seems satisfactory for these three examples.

5.1. *Test of literature models with experimental data*

The fragmentation threshold of off-centre binary collisions of drops of the same liquid can be derived from the surface energy balancing the rotational energy. This corresponds to the approach of Brazier-Smith *et al.* (1972) and yields a critical impact parameter proportional to the inverse of the Weber number, $X_{cr} \approx We^{-1}$. This model was developed for inviscid fluids. An alternative to this theoretical fragmentation limit has been proposed by Jiang *et al.* (1992), in which the surface energy is balanced by a viscous dissipation analogous to the friction observed between two solids sliding on top of each other. This second approach leads to an evolution of the critical parameter as $X_{cr} \approx We^{-1/2}\,(1 + kOh)$, where k is a constant adjusted by experimental data to give more or less weight to the Ohnesorge number Oh.

To test these models with the experimental data for binary collisions of drops of immiscible liquids, we collect from an (X, U) nomogram of our experiments a series of X_{cr}, U values corresponding to the fragmentation studied. As the wetting properties of our liquid combinations are similar, the Weber number can be reduced to U^2, and the two theoretical models can be rewritten as

$$X_{cr} \approx \frac{A}{U^2}, \tag{5.1}$$

$$X_{cr} \approx \frac{B(\mu)}{U}, \tag{5.2}$$

where A is a constant with dimension m^{-2} s^2, and the function B of the liquid viscosity has the dimension m s^{-1}. We compare some of our data to equations (5.1) and (5.2) in figure 17.

We see that the model (5.1) developed by Brazier-Smith *et al.* for inviscid liquids is not in good agreement with our experimental data. The second scaling law (5.2), derived by Jiang *et al.* (1992) for viscous liquids, does not really show better agreement. These observations encourage us to reconsider the variables used to describe this type of fragmentation. We especially note that the drops undergoing off-centre collisions are strongly distorted, and, if we furthermore admit – like Brazier-

https://doi.org/10.1017/jfm.2012.94 Published online by Cambridge University Press

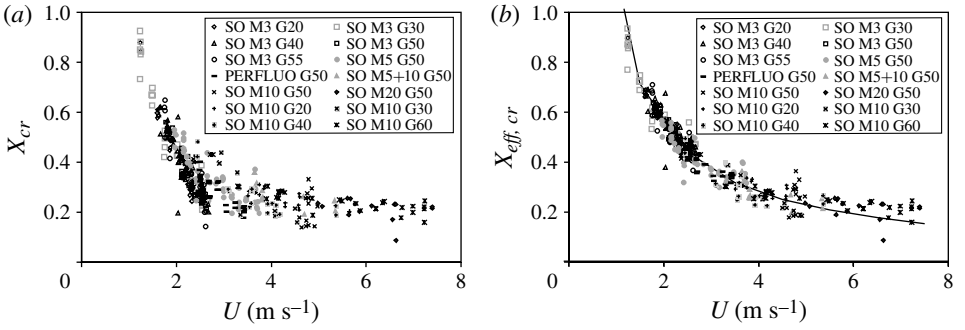


FIGURE 18. (*a*) The critical impact parameter X_{cr} for stretching separation as a function of the relative drop velocity U for several liquid combinations. (*b*) The critical effective impact parameter $X_{eff,cr}$ as a function of U. The correction applied makes the data collapse on a single curve corresponding to $X \approx 1/U$.

Smith *et al.* – that part of the kinetic energy is turned into rotation energy, it appears reasonable to introduce an 'effective' impact parameter, X_{eff}.

5.2. *Development of a modified impact parameter*

To empirically construct this new variable, we take into account the following three experimental facts:

(i) when U tends to 0, X_{eff} tends to X. Indeed, when the relative velocity is small, the impact is not strong enough to substantially distort the drops or to generate a strong rotation;

(ii) when X tends to 1, X_{eff} tends to X. Here, again, the interaction between the two drops is not strong enough to make any important difference between X_{eff} and X;

(iii) when X tends to 0, $X_{eff} - X$ increases with U.

Based on these requirements we propose expressing X_{eff} as

$$X_{eff} = X + (1 - X)\,\frac{U}{U^*}, \tag{5.3}$$

where U^* is an empirically determined constant with the dimension of a velocity. For validating this approach, we decided to use the more viscous combinations of liquids (SO M20–G50 and SO M10–G60) as a reference. In other words, no correction is applied to the impact parameter for these liquid pairs: the viscosities of the two liquids are in both cases large enough to keep the distortion small.

This transformation allows us to bring together all the data along a single curve corresponding to $X_{eff,cr} \approx 1/U$. This result is shown in figure 18, where the evolution of X_{cr} and $X_{eff,cr}$ with U is plotted. It is seen that the dependence of the critical impact parameter on the impact velocity remains a $1/U$ law, as found by Jiang *et al.* (1992), provided that the critical impact parameter is represented by its effective form given by (5.3). We deduce that the introduction of this effective impact parameter accounting for distortion and rotation of the drops is a promising way to construct a unique fragmentation limit and describe the various behaviours observed with a single law.

To take this concept further, we consider the evolution of the empirically determined constant U^* with the liquid viscosity. As shown in figure 19, where the evolution of U^* with different viscosities is plotted, the correction applied to the measured impact

https://doi.org/10.1017/jfm.2012.94 Published online by Cambridge University Press

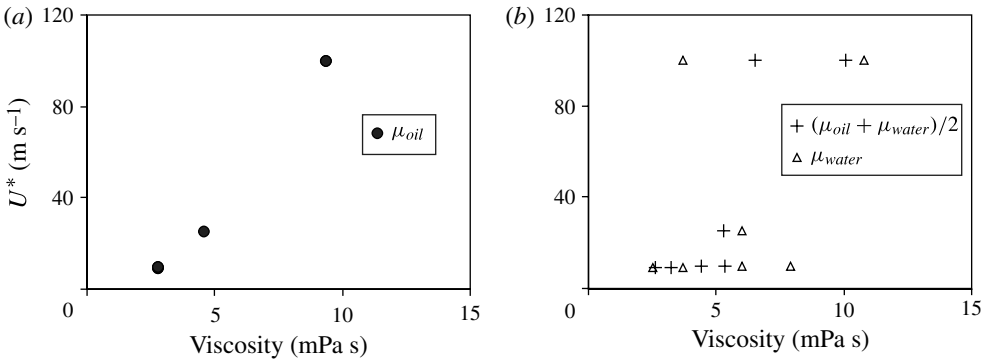


FIGURE 19. The reference velocity U^* as a function of the oil viscosity (*a*), and of the aqueous solution and of the average of the two (*b*). We note that only the oil viscosity yields a monotonic trend. The more viscous the oil, the less important the correction in (5.3).

parameter is a monotonic function of the oil viscosity. This result is in good agreement with the experimental observation showing a liquid ligament principally consisting of oil, which can be explained as a consequence of the stronger ability of oil to distort in comparison with the aqueous solutions of higher surface tension. We also note that the correction is the less important, the more viscous the oil. This last remark indicates, as expected, that the distortion of the drops increases when the drops are less viscous.

5.3. *Conclusions on the fragmentation after off-centre collisions*

The description of the fragmentation threshold for off-centre collisions of immiscible liquid drops is not possible with the models known from the literature. Moreover, the data collected for immiscible liquid drop collisions clearly show a variety of phenomena for different combinations of liquids. In this context, our new approach to introduce a modified, effective impact parameter, taking into account the distortion of the drops, seems to be very promising. We have shown that this operation can easily bring together all the data along a single curve. This correction is found to be less important for more viscous liquids. It also appears, as for head-on fragmentation, that the oil plays a stronger role than the aqueous solutions. The modification applied to the measured impact parameter indeed only depends on the oil viscosity, which is consistent with the finding from our experiments that liquid filaments formed by the off-centre collisions mainly consist of oil.

6. Conclusions

We have investigated the onset of fragmentation after binary collisions of drops of immiscible liquids. The experimental results obtained for a wide range of liquids are presented and tested against theoretical and empirical models.

For the head-on configuration, the collision process is found to be similar to a succession of compression and relaxation of the drops. The fragmentation criterion can be reduced to the well-known Rayleigh criterion for capillary instability. As for collisions of drops of the same liquid, the first period of the collision, during which the drops are distorted to form a lamella surrounded by a rim, generates inertial energy losses. We interpret this phenomenon as the consequence of the formation of flow fields inside the drops. The losses are found to be more important in the case of immiscible liquids than for drops of the same liquid, which is consistent with a

https://doi.org/10.1017/jfm.2012.94 Published online by Cambridge University Press

difference in the respective flow fields. In contrast to binary collisions of drops of the same liquid, for the liquids investigated here, the viscous dissipation of the second phase of the process is confined to the oil film and can therefore be easily expressed using the analogy with the relaxation of an encapsulated drop. For drops of the same liquid, literature data show two regimes depending on the importance of the viscous compared to the oscillation time scales. This transition could also exist for immiscible liquids in viscosity ranges not studied in our experiments so far.

For off-centre collisions, existing models (Brazier-Smith *et al.* 1972; Jiang *et al.* 1992) turned out to be unable to represent the experimental limits satisfactorily. Moreover, we observed that the critical impact parameter for stretching separation could not be represented by a single scaling law. To overcome this difficulty, we introduce a modified impact parameter, taking into account the distortion and rotation of the drops upon impact. Such an empirical effective parameter allows one to make all the data collapse on a single curve. As expected, the importance of drop distortion is found to increase as the viscosity decreases. In fact, the correction turns out to be a function of the oil viscosity alone, which is in good agreement with the fact that ligaments formed by off-centre collisions in our experiments consist of oil only. We believe that this new approach should lead the way to a single fragmentation law for all off-centre collisions with miscible or immiscible liquids.

Acknowledgements

The authors gratefully acknowledge M. Adler for her support as well as several funding sources: the Hubert Curien Program AMADEUS 2009 from the French Ministry of Foreign Affairs and the Austrian ÖAD and the European COST Action P21 – Physics of Droplets. Financial support from the Steiermärkische Landesregierung for C.P. is gratefully acknowledged. We wish to thank the institute CVTUT of Graz University of Technology for support in the measurements of interfacial tensions.

REFERENCES

ASHGRIZ, N. & POO, J. Y. 1990 Coalescence and separation in binary collisions of liquid drops. *J. Fluid Mech.* **221**, 183–204.

BARTOLO, D., JOSSERAND, C. & BONN, D. 2005 Retraction dynamics of aqueous drops upon impact on non-wetting surfaces. *J. Fluid Mech.* **545**, 329–338.

BIANCE, A.-L. 2004 Gouttes inertielles: de la caléfaction à l'étalement. PhD thesis, Université Paris VI.

BIANCE, A. L., CHEVY, F., CLANET, C., LAGUBEAU, G. & QUÉRÉ, D. 2006 On the elasticity of an inertial liquid shock. *J. Fluid Mech.* **554**, 47–66.

BRAZIER-SMITH, P. R., JENNINGS, S. G. & LATHAM, J. 1972 The interaction of falling water drops: coalescence. *Proc. R. Soc. Lond.* A **326**, 393–408.

BRENN, G., DURST, F. & TROPEA, C. 1996 Monodisperse sprays for various purposes – their production and characteristics. *Part. Part. Syst. Charact.* **13**, 179–185.

BRENN, G. & KOLOBARIC, V. 2006 Satellite droplet formation by unstable binary drop collisions. *Phys. Fluids* **18**, 087101.

BRENN, G., VALKOVSKA, D. & DANOV, K. D. 2001 The formation of satellite droplets by unstable binary drop collisions. *Phys. Fluids* **13** (9), 2463–2477.

CHEN, R.-H. 2007 Diesel-diesel and diesel-ethanol drop collisions. *Appl. Therm. Engng* **27**, 604–610.

CHEN, R.-H. & CHEN, C.-T. 2006 Collision between immiscible drops with large surface tension difference: diesel oil and water. *Exp. Fluids* **41**, 453–461.

https://doi.org/10.1017/jfm.2012.94 Published online by Cambridge University Press

CHU, L.-Y., UTADA, A. S., SHAH, R. K., K.IM, J.-W. & WEITZ, D. A. 2007 Controllable monodisperse multiple emulsions. *Angew. Chem. Intl Ed.* **46**, 8970–8974.

CLANET, C., BGUIN, C., RICHARD, D. & QUÉRÉ, D. 2004 Maximal deformation of impacting drop. *J. Fluid Mech.* **517**, 199–208.

EGGERS, J., FONTELOS, M. A., JOSSERAND, C. & ZALESKI, S. 2010 Drop dynamics after impact on a solid wall: Theory and simulations. *Phys. Fluids* **22**, 062101.

ESTRADE, J.-P., BERTHOUMIEU, P., LAVERGNE, G. & BISCOS, Y. 1998 Experimental investigation of dynamic binary collision of various liquids. In *8th International Symposium on Flow Visualization* (ed. G. M. Carlomagno & I. Grant).

GAO, T.-C., CHEN, R.-H. & LIN, T.-H. 2005 Collision between an ethanol drop and a water drop. *Exp. Fluids* **38**, 731–738.

GOTAAS, C., HAVELKA, P., JAKOBSEN, H. A., SVENDSEN, H. F., HAASE, M., ROTH, N. & WEIGAND, B. 2007 Effect of viscosity on droplet-droplet collision outcome: Experimental study and numerical comparison. *Phys. Fluids* **19**, 102106.

GOUBAULT, C., PAYS, K., OLEA, D., GORRIA, P., BIBETTE, J., SCHMITT, V. & LEAL-CALDERON, F. 2001 Shear rupturing of complex fluids: Application to the preparation of quasi-monodisperse water-in-oil-in-water double emulsions. *Langmuir* **17** (17), 5184–5188.

JIANG, Y. J., UMEMURA, A. & LAW, C. K. 1992 An experimental investigation on the collision behaviour of hydrocarbon droplets. *J. Fluid Mech.* **234**, 171–190.

MARMOTTANT, P. & VILLERMAUX, E. 2004 Fragmentation of stretched liquid ligaments. *Phys. Fluids* **16**, 2732–2741.

NOTZ, P. K. & BASARAN, O. A. 2004 Dynamics and breakup of a contracting liquid filament. *J. Fluid Mech.* **512**, 223–256.

OKUMURA, K., CHEVY, F., RICHARD, D., QUÉRÉ, D. & CLANET, C. 2003 Water spring: A model for bouncing drops. *Europhys. Lett.* **62** (2), 237–243.

OKUSHIMA, S., NISISAKO, T., TORII, T. & HIGUCHI, T. 2004 Controlled production of monodisperse double emulsions by two-step droplet breakup in microfluidic devices. *Langmuir* **20** (23), 9905–9908.

PLANCHETTE, C., LORENCEAU, E. & BRENN, G. 2010 Liquid encapsulation by binary collisions of liquid drops. *Colloids Surf.* A **365**, 89–94.

QIAN, J. & LAW, C. K. 1997 Regimes of coalescence and separation in droplet collision. *J. Fluid Mech.* **331**, 59–80.

RAYLEIGH, LORD 1879 On the capillary phenomena of jets. *Proc. R. Soc. Lond.* **29**, 71–97.

RICHARD, D., CLANET, C. & QUÉRÉ, D. 2002 Contact time of a bouncing drop. *Nature* **417**, 811.

TONG, A. Y. & WANG, Z. 2007 Relaxation dynamics of a free elongated liquid ligament. *Phys. Fluids* **19** (9), 092101.

UTADA, A. S., LORENCEAU, E., LINK, D. R., KAPLAN, P. D., STONE, H. A. & WEITZ, A. 2005 Monodisperse double emulsions generated from a microcapillary device. *Science* **308**, 537–541.

VILLERMAUX, E. & BOSSA, B. 2011 Drop fragmentation on impact. *J. Fluid Mech.* **668**, 412–435.

VINCENT, F., LEGOFF, A., LAGUBEAU, G. & QUÉRÉ, D. 2007 Bouncing bubbles. *J. Adhes.* **83**, 897–906.

WILLIS, K. & ORME, M. 2000 Experiments on the dynamics of droplet collisions in a vacuum. *Exp. Fluids* **29** (4), 347–358.

https://doi.org/10.1017/jfm.2012.94 Published online by Cambridge University Press